FIELD MAPPING OF WETTING FRONT USING GROUND PENETRATING RADAR UNDER UNIFORM AND NON-UNIFORM WETTING

D.M.C.S. Mimrose[1], L.W. Galagedara[2*], and G.W. Parkin[3]

[1]Postgraduate Institute of Agriculture, University of Peradeniya, Peradeniya, Sri Lanka
mimrose124@gmail.com

[2]Department of Agricultural Engineering, University of Peradeniya, Peradeniya, Sri Lanka
lgalaged@pdn.ac.lk

[3]School of Environmental Sciences, University of Guelph, Guelph, ON, Canada
gparkin@uoguelph.ca

Abstract: This research was carried out to develop 2D and 3D maps of a wetting front and to identify potential preferential flow areas using Ground Penetrating Radar (GPR). GPR grid data were collected during uniform and non-uniform wetting experiments. Maps were prepared for different depth profiles for each data set, collected at different time intervals after starting water application. The wetting front had reached a maximum depth of 0.45–0.50 m within 25 hours of continuous wetting based on 2D and 3D GPR images. In the uniform wetting experiments, potential preferential flow zones could be identified in 2D and 3D maps.

Key Words: Ground penetrating radar, wetting front, preferential flow, water content

1. INTRODUCTION

A wetting front can be defined as a thin transition zone where the soil water content changes from its initial low value to a higher value at the leading edge of an infiltration event. Usually the process of water infiltration in soil from a point source creates an onion-shaped wetting front that slowly propagates vertically and horizontally (Gvirtzman *et al*., 2008). Instability in the wetting front may lead to the creation of preferential flow pathways (Raats, 1973). Preferential flow refers to the uneven and often rapid movement of water and solute through porous media, while matrix flow is a relatively slow and even movement of water and solute through soil (Singh, 1995). Once preferential flow paths have formed, the soil no longer impedes infiltration of water; additional precipitation tends to infiltrate through the pre-existing preferential paths, which have been wetted before (Dekker *et al.*, 2001). Thus, dry zones tend to persist due to their water repellent character and their low hydraulic conductivity. Research conducted by Mowjood *et al.* (2005) using crack measurements and water advance front sensors shows that water can move rapidly through a subsurface crack network, with the cracks acting as preferential flow pathways. Most models which are used to simulate water and solute transport through the unsaturated zone assume uniform downward movement of the wetting front parallel to the soil surface during an infiltration event. But this assumption is not valid for most of the cases described above when there is preferential flow.

Preferential flow is often considered to facilitate groundwater contamination. Identifying and mapping of preferential flow areas can help in minimizing groundwater contamination by adopting appropriate soil and water management strategies in the identified areas. t is necessary to understand how preferential flow pathways develop in the soil subsurface both vertically and horizontally (Galagedara, 2003). Densely sampled soil moisture data required for mapping cannot be obtained through conventional methods such as gravimetric, time domain reflectometry (TDR), capacitance-based sensors or neutron scattering. On the other hand, the GPR method has been identified as an efficient method to measure soil moisture variability over large areas (Grote *et al*., 2003; Hubbard *et al*., 2002; Huisman *et al*., 2001) with larger sampling volume, non-intrusive sampling and less time consumption than other methods. In addition, researchers have used GPR to characterize hydrological processes in the vadose zone including mapping of wetting front movements and identify potential preferential flow pathways (Daniels *et al*., 1994; Galagedara *et al*., 2005; Gish *et al*., 2002; Rucker and Ferre, 2002; Saintenoy *et al*., 2007; Vellidis *et al*., 1990).

The main objective of this research was to develop 2D and 3D maps of a wetting front during infiltration from a combined line and point source and identify the potential preferential flow zones

within the wetted soil under field conditions using GPR. A second objective was to compare wetting front configurations for two different methods of applying water to the soil surface. As explained below, 2D and 3D maps of soil water distribution were prepared using GPR data collected in a grid of 2.0 m x 2.5 m with two different methods of water application with different water application rates and durations. Finally, to assess the importance of characterizing the 2D and 3D nature of the infiltration, the patterns of wetting front advance measured by GPR were compared against estimates of the advance of the wetting front for similar experimental conditions using a 1D infiltration model (HYDRUS 1D).

2. MATERIALS AND METHODS

2.2 The GPR Method

Researchers have put forth GPR as a sensitive shallow earth mapping technique that can be potentially used to identify paths for preferential flow by monitoring soil water movement in the vadose zone (Daniels *et al*., 1994; Freeland, 2006; Kishel and Gerla, 2002; Vellidis *et al*., 1990). In a GPR survey conducted in a uniformly wetted land by Vellidis *et al*. (1990), it was evident that the shapes of the wetting front and water application uniformity curves are mirror images of each other. In other studies, high water content zones (possibly preferential flow zones) were identified by a borehole GPR survey conducted during wetting and drying conditions in a well drained sandy loam soil (Galagedara *et al*., 2003; Parkin *et al.*, 2000). Research conducted by Saintenoy *et al*. (2007) showed that surface-based GPR data provide valuable information to study the evolution of a water bulb with hydrodynamic modeling. Research done in sandy soils using GPR have visualized discrete wetting front and preferential flow paths (Harari, 1996). Simulated wetting fronts were observed in sand tanks in the laboratory using GPR (Seung-Yeup *et al*., 2007). For this study, the PulseEKKO PRO GPR system was used and data collection procedure, survey method, equipment settings etc., were done based on the operation manual (Sensor and Software Inc., 2006). Site selection was done through a background survey conducted using both 100 MHz and 200 MHz GPR antennas.

2.2 Location

Research was carried out at the Meewathura research station of the Department of Agricultural Engineering, University of Peradeniya, Sri Lanka (7^0 15' 10.97" N, 80^0 35' 42.57" E, and Elevation 475 m). A study area of 2.5 m x 2.0 m was selected (Fig. 1) having nearly uniform, flat ground with nearly homogeneous soils in the subsurface down to about 1.5 m depth.

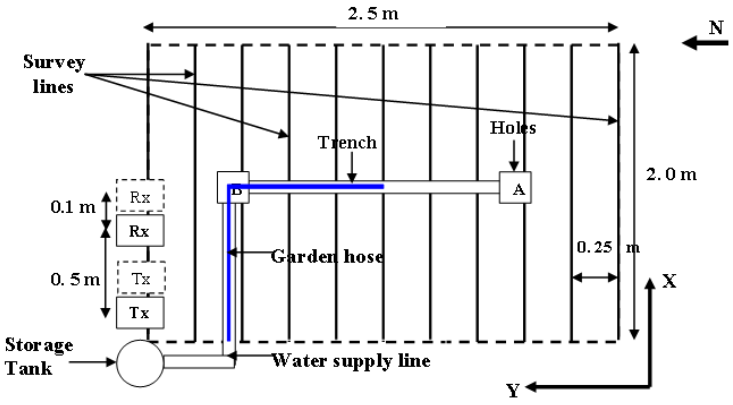

Fig. 1: Schematic diagram of the experimental area showing water supply system and GPR survey lines
Tx: Transmitter antenna; Rx: Receiver antenna.

Having uniform subsurface conditions is potentially important to help observe the wetting front clearly with the GPR method as the number of wave reflections of soil horizon boundaries is minimized. The major soil type in the area is sandy clay loam originating from alluvial deposits. Undisturbed soil samples were collected from the study site at three different depths with two replicates. These samples were used to estimate the soil physical properties using standard laboratory procedures. Physical properties of the soil in the study area are given in Table 1.

Table 1: Measured soil physical and hydraulic properties of the field site

Soil Type and Depth (cm)	Sand (%)	Silt (%)	Clay (%)	OM† (%)	Porosity (%)	BD‡ (g/cm^3)	Ks§ (m/sec)
0-15 (SCL) #	59.4	8.6	32.0	3.14	43.2	1.54	3.5E-07
15-30 (SC) #	60.0	5.0	35.0	n/a	46.3	1.49	1.2E-05
30-40 (SC) #	47.0	16.0	37.0	1.54	45.3	1.45	1.1E-06

†Organic Matter; ‡Bulk Density; §Saturated Hydraulic Conductivity; ¶Sandy Clay Loam; #Sandy Clay

2.3 Experiment 1

Water application to the study area was carried out from two square-shaped of 15-cm in size and 20-cm in depth holes (A and B) and a connecting trench of 5-cm width and 10-cm depth (Fig. 1). A garden hose (1.27 cm diameter) was laid over half of the trench as a water source for the trench and holes A and B. (Fig. 1). Water discharged from the end of the garden hose to fill the trench and holes and expected that the holes would generate preferential flow beneath them. The trench and the two holes (A and B) were back filled with stone chips (5-10 mm diameter) in order to obtain good ground coupling of GPR antennas. Fresh water was applied at an average rate of 4.6 mL/sec for 21.50 h of total time duration. Water application rate was obtained by measuring the volume of water collected at a known time period. A tightly-controlled water application rate was not possible since the water supply hose was directly connected to a garden tap and water pressure was varying during the day.

2.4 Experiment 2

In this case, a perforated PVC pipe of 1.27 cm diameter and 1.5 m length was placed in the trench to supply water more uniformly than the garden hose. Two sets of holes were made on both sides along the horizontal axis of the pipe. Holes were placed keeping a constant interval distance of 5.0 cm to ensure uniform water supply along the trench. Under experiment 1, uniform water application was not possible because water was applied from one location of the trench. A PVC pipe having the same diameter as the perforated pipe was buried in the soil at 10-cm depth to

supply water from the tank to the perforated pipe. The trench and two holes (A and B) were filled with coarse sand after placing the pipe. Water was applied at a rate of 24 mL/sec for 25 h of total time duration. A much more uniform water application rate could be obtained during this experiment compared to experiment 1 by having a constant water head tank (Fig. 1) as the source of water instead of the tap.

In both experiments, GPR grid surveys were carried out using 200-MHz antenna employing the reflection survey method (Annan, 2005; Smith *et al*., 1992; Hunaidi *et al*., 1998). GPR surveys were carried out having 0.25-m line spacing, 0.5-m antenna separation and 0.1-m step size as shown in Fig. 1. GPR grid survey lines (eleven lines) were oriented from West to East (X direction) and each survey was carried out beginning from the survey line in the South to North (Y direction) as shown in Fig. 1. Data collection began 30 min. after starting water application in both experiments. Four data sets were collected during experiment 1, while six data sets were collected during experiment 2. Background surveys were carried out before starting the water application in both experiments in order to assess the effect of water application and changes in the wetting patterns with depth. EKKO Delux, EKKO View and EKKO Mapper (Sensors and Software Inc.) and Voxler 3D (Golden Software Inc) computer softwares were used to develop and interpret 2D and 3D maps of the subsurface soil water content distribution collected at the field.

2.5 Simulation of wetting front advance using HYDRUS 1D

Wetting front advancement was simulated using HYDRUS 1D (Šimůnek *et al*., 2005) for a three layer (Table 1) soil profile of 120-cm thickness. During this simulation, data from Table 1 were used for three different soil layers. The thickness of the third layer was considered from 30 to 120 cm since soil properties below 40 cm depth was not obtained. During the simulation, water flow was considered as one dimensional (vertical). Calculations were done for 25 h of total time period starting from 0.5 h. Changes in wetting front depth in the profile were simulated 9 times at different elapsed times from starting of water application. Soil textural values and bulk density values for three different layers were used to predict soil hydraulic parameters in HYDRUS 1D (Table 1). Van-Genuchten- Mualem model was used in parameter estimation for unsaturated water flow simulation. Simulation was done using two upper boundary condition values. For the first run, the initial upper boundary conditions (matrix potential) were set as 0 kPa for 0-1.0 cm layer and -1000 kPa for 1.0-120.0 cm layer assuming the saturation condition at the trench. For the second run, the initial upper boundary conditions were set as -10 kPa for 0-1.0 cm layer and -1000 kPa for 1.0-120.0 cm layer assuming the near saturation condition at the trench. This second run was done because the real saturation condition is not generally achieved during field conditions. And also, due to comparatively lower hydraulic conductivity of the first layer, the water application rate had to be kept at a lower rate in order to avoid flooding conditions which can affect GPR antennas. So that, we assumed the second run was more closely representing the actual field situation. As for both runs, the lower boundary condition was kept as free drainage.

3. RESULTS AND DISCUSSIONS

3.1 Experiment 1

Two-dimensional images showing relative strength of reflected signal at different soil depths at different time intervals beneath the grid area were prepared using EKKO Mapper (SSI) software. The velocity of the radar wave could not be estimated accurately due to difficulty in separating the direct ground wave (DGW) from other waves collected using common mid-point (CMP) survey data, during this experiment. The average radar wave velocity of 0.10 m/ns was assumed in developing these wetting from maps. The disturbances masking the DGW could potentially be due to environmental noise from nearby power lines and or metals presence in the vicinity. Fig. 2 shows variation of reflected wave strengths at different times at 0.20 – 0.30 m and 0.25 – 0.30 m depths. The expected preferential flow areas in holes A and B could not be observed, potentially due to uneven water application to the trench. However, according to Fig. 2d, three preferential wettings could be observed. The most dominant wetting can be seen at 1.25 mN line (just south of B hole) which is just below the water application point (Fig. 1). It is clear that the wetting front had reached at 0.25 – 0.30 m depth after 7 hours of wetting (Fig. 2e) and the

signal strength increases after 7 hours of wetting (Fig. 2d) due to increase of moisture content with continued infiltration. However, as shown in Fig. 2b, the wetting is more dominant north of hole B after 40 min of wetting compared to other areas including the infiltrating point.

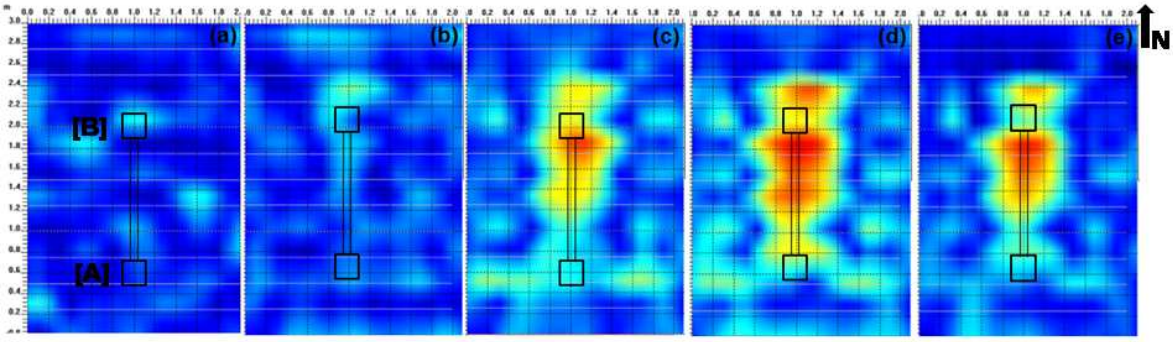

Fig. 2: Maps of GPR reflected signal strength showing changes in wetting pattern in 0.20 - 0.30 m depth slice under experiment 1 conditions. (a): background; (b) after 40 min; (c) after 5 h; (d) after 7 h; (e) 0.25 – 0.30 m depth slice after 7 h.
(Strength of the reflected signal increases from blue→green→yellow→orange→red).

According to Fig. 3, the wetting pattern has developed horizontally (horizontal seepage) as well, when compared with the same depth slice (Figs. 3b and 3c). However, the horizontal seepage is less in Fig. 3d compared to Fig. 3c. This variation could be due to the variability of wetting due to the effect of gravity and negative pressure potential. When the soil is dry, negative pressure dominates the water flow where wetting font advancement can be expected both horizontally and vertically. With continued wetting negative pressure decreases and gravity dominates in wetting where vertical movement of water is prominent at the given depth compared to horizontal movement. In addition, water application method and rate directly connecting to a garden tap during the experiment 1 could also have created this variation. Overall, it is clear that both vertical and horizontal wetting had occurred during this experiment and sharp wetting fronts become less well defined with time when comparing Figs. 3d and 3e.

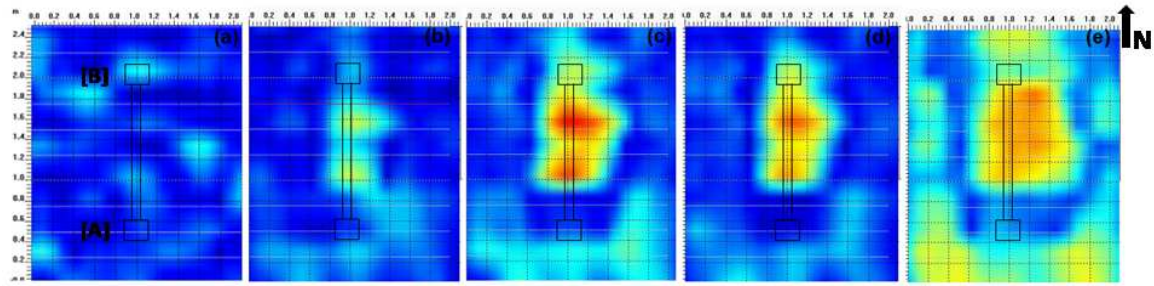

Fig. 3: Maps of GPR reflected signal strength showing changes in wetting pattern in 0.20- 0.30 m depth slice under experiment 1 conditions. (a): background; (b) after 30 min; (c) after 1 h 30 min; (d) after 2 h 30 min (e) after 21 h.
(Strength of the reflected signal increases from blue→green→yellow→orange→red).

In the 3D images shown in Fig. 4, the middle vertical plane is located at the same location as the water application trench in the Y direction of the grid (Fig. 1). Changes in wetting pattern can be observed in the middle vertical plane with time in comparison with the 3D image produced for the background survey (Fig. 4). Two prominent wetted areas can be observed in the 3D image after 30 min. representing the two potential preferential flow areas found in 2D images at the 1.0 and 1.6 m N lines (Fig. 3c). After 21.0 h, applied water has concentrated in a depth range about 0.20 – 0.30 m, and has not reached a depth below 0.50 m. Accumulation of water in 0.20 – 0.30 m soil profile was observed in 2D images as well (Figs. 2d, 3c and 2d).

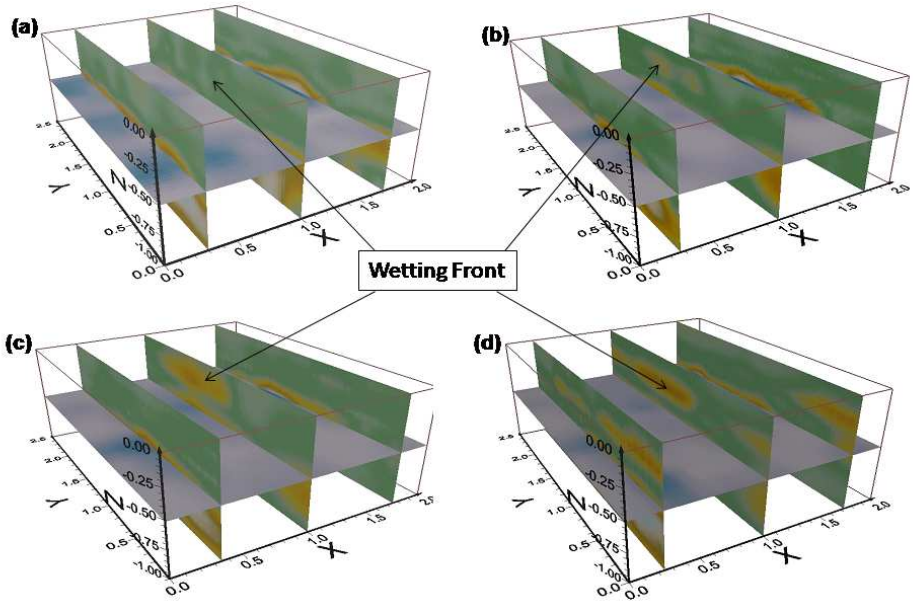

Fig. 4: 3D images of the GPR reflected signal strength beneath the study area at the indicated elapsed times after starting water application under experiment 1 condition. Three vertical slices are at 0.5, 1.0 and 1.5 m North lines where the water was applied at 1.0 m North line (Arrows show the development of the wetting front with time at the centre line). (a) background; (b) after 30 min; (d) after 1 h and 30 min; (d) after 21 hr.

3.2 Experiment 2

In Fig. 5, nearly uniform wetting could be observed along the trench when compared with images produced in the previous experiment. A stronger reflected signal indicating the wetting pattern with red color is visible than in figures obtained in the previous experiment. It is probably due to the increased volume of applied water. A preferential flow area is visible near the North end of the trench (Fig. 5). This clear preferential flow area is prominent at the early stage of water application and reached down to about 0.35 - 0.40 m depth within 30 min. (Fig. 5c). The wetting pattern could be clearly observed up to the 0.45 - 0.50 m depth slice with 0.100 m/ns velocity.

The wetting pattern is prominent in the middle area of the trench in experiment 1 as water was applied from the middle area. In experiment 2, the wetting pattern has spread throughout the whole length of the trench. The maximum depth of water infiltration of 0.45 - 0.50 m was achieved within 1 h at a water application rate of 24 mL/sec with an assumed velocity of 0.100 m/ns. Actual velocity could not be estimated due to difficulty of producing a velocity profile for the study area using the DGW method. This depth may slightly change with the actual wave velocity.

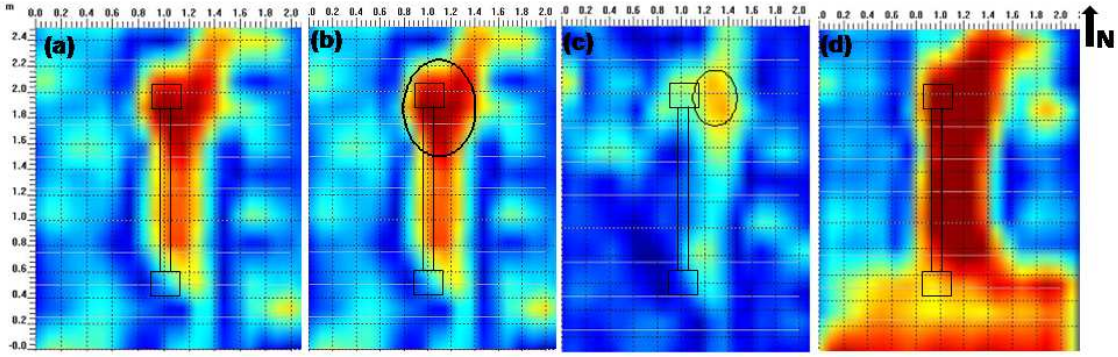

Fig. 5: Maps of GPR reflected signal strength showing changes of wetting pattern and potential preferential flow areas under experiment 2 conditions. (a) after 30 min at 0.20-0.30 m depth; (b) after 30 min at 0.30-0.40 m depth; (c) after 30 min at 0.35-0.40 m depth; (d) after 2 h at 0.20-0.30 m depth.
(Strength of the reflected signal increases from blue→green→yellow→orange→red)

3.3 Simulated depths of wetting front using HYDRUS 1D

According to derived hydraulic properties during the HYDRUS 1D simulation, the third layer has the highest saturated soil water content (porosity) and the lowest saturated hydraulic conductivity (Ks). However, according to the measured values, the highest Ks value is found at the middle layer followed by the lower layer and upper layers, respectively (Table 1). As for the saturated water content values (porosity), all the values derived by HYDRUS 1D were lower compared to measured values. The effect of different hydraulic properties at different layers on the simulated wetting front can be seen in Fig. 6. It is clear that none of the layers reached the saturated water content under the second run potentially due to the lower boundary of free drainage and lower water application rate. However, it can be seen in Fig. 6b that the first layer water content had reached to steady state water content of 0.38-0.39 m^3/m^3 of soil (the saturated water content is 0.406 m^3/m^3 of soil).

Applying the HYDRUS 1D model to the experiment 2 conditions, the wetting front has reached up to about 35 cm depth in 10 h and about 80 cm depth in 25 h for the first model run (Fig. 6a). The wetting front has reached up to about 15 cm depth in 10 h and about 30 cm depth in 25 h for the second model run (Fig. 6b). When comparing the results of the first model run with wetting front depth observed using GPR,

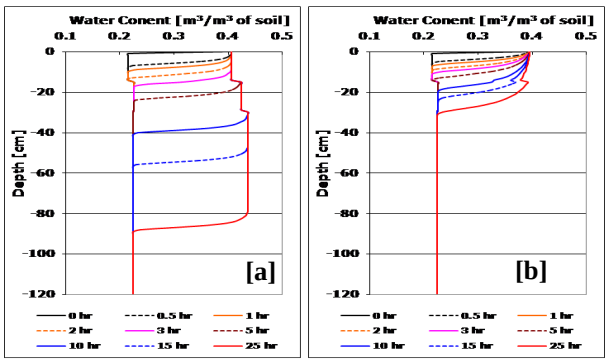

Fig. 6: Simulated depths of wetting front using Hydrus 1D under conditions of experiment 2.
(a): Constant pressure of the upper boundary = 0 kPa
(b): Constant pressure of the upper boundary = -10

It is clear that the first model run resulted in an overestimation of the wetting front advancement. However, the second model run gives comparatively better prediction of the wetting front advancement with the GPR method. In the second experiment, the average wetting front obtained from the GPR method is around 0.25-0.30 m even though the maximum depth observed was 0.40 m (Fig. 5c). This maximum depth is reached after 25 hours of wetting potentially due to preferential flow and the average depth of wetting along the entire trench could be considerably lower. Variation in physical properties along the soil profile govern actual wetting front advancement while the assumed homogeneous properties along the trench length in the simulation might have affected the slight differences in the simulated wetting front advancement and maximum wetting depth observed in the GPR method. It can be revealed that the GPR observed average wetting depth could also be simulated using HYDRUS 1D. However, slight differences between the observed wetting front and simulated wetting front could be due to the differences in soil hydraulic properties as well as variation of the GPR wave velocity with increasing water content which was not considered in preparation of wetting front advancement maps.

4. CONCLUSIONS

A maximum wetting front infiltration depth of 0.40 - 0.45 m was achieved at a water application rate of 24 mL/sec within 1.0 h based on the observation made by the GPR method. This depth of penetration was much greater than the depth predicted by HYDRUS 1D, demonstrating the importance of preferential flow under the site and experimental conditions of this study. Simulation exercise revealed that upper soil layer reached steady state water content within 25 hours of water application. This study has shown that the surface GPR method can be satisfactorily used to identify wetting patterns and potential preferential flow areas under field conditions. Both 2D and 3D maps of the pattern of wetting beneath an infiltration trench were successfully developed. Preferential flow zones were visible in both map configurations as zones of relatively high wave reflection. Preferential flow was observed under both experimental designs, but a uniform wetting is recommended instead of wetting from one location as used in this study. A second recommendation based on this work is that the GPR grid data should be collected at shorter time intervals during the early stage of water application to observe a clear wetting pattern. Similar study under more controlled condition can also be recommended and validation should be done using a 2D simulation (HYDRUS 2D) model to catch the horizontal variation of the soil hydraulic properties.

ACKNOWLEDGEMENTS

Authors wish to acknowledge the National Research Council (NRC) of Sri Lanka for financial support given to purchase the GPR equipment and conduct field research (Grant Number NRC/05-38). Dr. van Genuchten, M. Th. for providing HYDRUS 1D free of charge. Senani gave an excellent support during field works.

REFERENCES

Annan A.P. (2005), "GPR Methods for Hydrogeological Studies in Hydrogeophysics", Springer Netherlands.

Daniels, J.J., Robrts R., Vendi, M. (1994), "Ground penetrating radar for the detection of liquid contaminants", *Journal of Applied Geophysics*, 33: 195-207.

Dekker, L.W., Ritsema, C.J., Oostindie K. (2001), "Wetting patterns and preferential flow in soils". *In: Proc. 2nd Int. Symp on Preferential Flow, Water Movement and Chemical Transport in the Environment*, pp. 85-88 D.D. Bosch and K.W. King. St. Joseph (Eds), Michigan 3-5 January 2001, Honolulu, USA.

Freeland, R.S., Odiambo, L.O., Tyner, J.S., Ammons, J.T., Write, W.C. (2006), "Non-intrusive mapping of near surface preferential flow", *Applied Engineering in Agriculture*, 22(2): 315- 319. American Society of Agriculture and Biological Engineers. ISSN. 0883-8542.

Galagedara, L.W. (2003), "The GPR direct ground wave method for soil moisture content estimation: Field experimental modeling (*Unpublished PhD thesis*)", University of Guelph, Canada.

Galagedara, L.W., Parkin, G.W., Redman, J.D., Endres, A.L. (2003). "Assessment of soil moisture content measured by borehole GPR under transient irrigation and drainage", *Journal of Environmental and Engineering Geophysics*, 8(2): 77-86.

Galagedara, L.W., Parkin, G.W., Redman, J.D., von Bertoldi P., Endres, A.L. (2005), "Field studies of the GPR ground wave method for estimating soil water content during irrigation and drainage", *Journal of Hydrology*, 301: 182-197.

Gish, D.W.P., Kung, K.J.S., Daughtry, C.S., Doolittle, J.A., Miller, P.T. (2002), "Evaluating use of ground penetrating radar for identifying subsurface flow pathways", *Soil Science Society of America*, 66: 1620-1629.

Grote, K., Hubbard, S., Rubin, Y. (2003), "Field-scale estimation of volumetric water content using ground-penetrating radar ground wave techniques", *Water Resources Research*, 39(11): 1321-1335.

Gvirtzman, H., Shalve, E., Dahan, O., Hazor, Y.H. (2008), "Large-scale infiltration experiments into unsaturated stratified loess sediments: monitoring and modeling", *Journal of Hydrology*, 394: 214-229.

Harari, Z. (1996), "Ground penetrating radar for imaging stratigraphic features and ground water sand dunes", *Journal of Applied Geophysics*, 36(1): 43-52.

Hubbard, S., Grote, K., Rubin, Y. (2002), "Mapping the volumetric soil water content of a California vineyard using high-frequency GPR ground wave data", *The Leading Edge*, June: 552-559.

Huisman, J.A., Sperl, C., Bouten, W., Verstraten, J.M. (2001), "Soil water content measurements at different scales: accuracy of time domain reflectometry and ground-penetrating radar", *Journal of Hydrology*, 245: 48-58.

Hunaidi, O., Giamou, P. (1998), "Ground penetrating radar for detection of leaks in buried plastic water distribution pipes", *In: Seventh International Conference in Ground Penetrating Radar*, Lawrence, Kansas, USA,

Mowjood, M.I.M., Pathmarajah, S., Rambanda, M. (2005), "Effect of cracks on water requirement for land soaking in lowland paddy cultivation", *Journal of Soil Science Society of Sri Lanka*, 17: 1-10.

Parkin, G., Redman, D., von Bertoldi, P., Zhang, Z. (2000), "Measurement of soil water content below a wastewater trench using ground penetrating radar", *Water Resources Research*, 36(8): 2147-2154.

Raats, P.A.C. (1973), "Unstable wetting fronts in uniform and non-uniform soils". *Soil Science Society America Journal*, 1973; 37: 681-685.

Rucker, D.F., Ferre, T.P. (2002), "Measuring the advance of a wetting front using cross-borehole GPR", *In: Ninth International Conference on Ground Penetrating Radar*, Koppenjan SK, Lee H (eds). Proceedings of SPIE 4758, 2002; 176-179. 176-180.

Saintenoy, A., Schneider, S., Tucholka, P. (2007), "Evaluating ground penetrating radar use for infiltration monitoring", *Vadose Zone Journal*, 7: 208-214.

SSI. (2006), PulseEKKO PRO users' guide, Sensors and Software Inc., Mississauga, ON, Canada.

Seung-Yeup, H., Yu-Sun, Jo, Heon-Cheol, Oh, Se- Yun, K., Young- Sik, K. (2007), "The laboratory scaled-down model of a ground-penetrating radar for leak detection of water pipes", .*Measurement Science and Technology*, 18: 2791-2799.

Šimůnek, J., van Genuchten, M.Th., Šejna, M. (2005), "The HYDRUS-1D Software Package for Simulating the One-Dimensional Movement of Water, Heat, and Multiple Solutes in Variably-Saturated Media", Department of Environmental Sciences, University of California Riverside, Riverside, California.

Singh, V.P. (1995), "Environmental Hydrology", *Springer*. pp 194-199.

Smith, D.G., Harry, M.J. (1992), "Ground-penetrating radar investigation of a Lake Bonneville deita, Provo level, Brigham City, Utah", *Geology*, 20: 1083-1086,

Vellidis, G., Smith, M.C., Thomas, D.L., Asmussen, L.E. (1990), "Detecting wetting front movement in a sandy soil with ground penetrating radar", *American Society of Agricultural Engineers*, 33(06):1867-1873.